Received: 19 May 2020 | Revised: 22 August 2020 | Accepted: 27 August 2020

DOI: 10.1096/fj.202001234R

RESEARCH ARTICLE

THE FASEB JOURNAL

Rspo1/Rspo3-LGR4 signaling inhibits hepatic cholesterol synthesis through the AMPKα-SREBP2 pathway

Shiying Liu[1] | **Yuan Gao**[1] | **Liping Zhang**[2] | **Yue Yin**[1] | **Weizhen Zhang**[1,2]

[1]School of Basic Medical Sciences, Peking University, Beijing, China

[2]Department of Surgery, University of Michigan Medical Center, Ann Arbor, MI, USA

Correspondence
Weizhen Zhang and Yue Yin, Department of Physiology and Pathophysiology, School of Basic Medical Sciences, Peking University Health Science Center, Beijing 100191, China.
Email: weizhenzhang@bjmu.edu.cn (W. Z.) and yueyin@bjmu.edu.cn (Y. Y.)

Funding information
National Key R&D Program of China, Grant/Award Number: 2017YFC0908900; National Natural Science Foundation of China, Grant/Award Number: 81730020 and 81930015; National Institutes of Health, Grant/Award Number: 1R01DK110273 and R01DK112755

Abstract

R-spondins (Rspos) are endogenous ligands of leucine-rich repeat-containing G-protein-coupled receptor 4 (LGR4). Rspos-LGR4 signaling plays important roles in embryogenesis, gastrointestinal homeostasis, and food intake. Here, we investigated the impacts of Rspos-LGR4 on hepatic cholesterol synthesis. Rspo1/3 and *Lgr4* knockdown mice were used to investigate the impacts of Rspo1/3-LGR4 on hepatic cholesterol synthesis. AMPKα agonist, antagonist, and shRNA were used to explore the downstream targets of Rspos-LGR4 signaling. In our study, we reported that LGR4, Rspo1, and Rspo3 were highly expressed in hepatocytes and their expressions were sensitive to energy states. Rspo1 and Rspo3 reversed OA-induced cholesterol synthesis, accompanying with increased the phosphorylation of AMPKα Thr172, reduced SREBP2 nuclear translocation, and *Srebf2* mRNA expression. Conversely, hepatic LGR4 knockdown increased hepatic cholesterol synthesis and decreased the phosphorylation of AMPKα both in vitro and in vivo. Activation or inhibition of AMPKα significantly abolished the effects of LGR4 deficiency or Rspos, respectively, on cholesterol synthesis. Knockdown of AMPKα1 or/and AMPKα2 repressed Rspos-induced inhibition on cholesterol synthesis. Our study indicates that Rspo1/Rspo3-LGR4 signaling in hepatocytes suppresses cholesterol synthesis via the AMPKα-SREBP2 pathway.

KEYWORDS

AMPK, cholesterol, LGR4, liver, R-spondins

1 | INTRODUCTION

Non-alcoholic fatty liver disease (NAFLD) is a set of metabolic disorders characterized by increased hepatic lipid deposit, including non-alcoholic fatty liver (NAFL), non-alcoholic steatohepatitis (NASH), and liver cirrhosis. NAFLD has become one of the most common chronic liver diseases worldwide.[1] Despite considerable efforts in the

Abbreviations: AMP, adenosine 5′-monophosphate; AMPKα, AMP-activated protein kinase α; ER, endoplasmic reticulum; FBS, fetal calf serum; GSK3β, glycogen synthase kinase 3β; HFD, high-fat diet; Insig, insulin-induced gene; LGR4, leucine-rich repeat G-protein-coupled receptor 4; NAFL, non-alcoholic fatty liver; NAFLD, non-alcoholic fatty liver disease; NASH, non-alcoholic steatohepatitis; NC, nitrocellulose; NCD, normal chow diet; OA, oleic acid; PA, palmitic acid; Rspos, R-spondins; SCAP, SREBP cleavage activation protein; SREBP2, sterol regulatory element-binding protein 2; S1P, site-1 protease; S2P, site-2 protease; SRE, sterol regulatory element; SREBP2-N, SREBP2 N terminus; WT, wild type.

Shiying Liu and Yuan Gao should be considered the joint first author.

study of NAFLD, its effective intervention remains limited. Researches have validated that the progression of NAFLD is accompanied by elevated cholesterol content in liver. In particular, the severity of NAFLD is positively correlated with increased hepatic synthesis of cholesterol.[2] Lipidomic analysis of NAFLD also revealed a stepwise increment of hepatic free cholesterol in NASH compared with NAFL.[3] Consistently, clinical studies suggested that pharmaceutical interventions of cholesterol synthesis or absorption significantly alleviate inflammation and fibrosis of NAFLD patients.[4,5] All these findings indicated that the intervention of cholesterol synthesis may also benefit the control of NAFLD, in addition to atherosclerosis.

The maintenance of hepatic cholesterol homeostasis depends on the balance between cholesterol synthesis and removal. Previous studies revealed that both extracellular signals and intracellular molecules contribute to the dynamic control of hepatic cholesterol metabolism.[6] One of the key intracellular modulators is a sterol regulatory element-binding protein 2 (SREBP2).[6] Encoded by the *Srebf2* gene, SREBP2 precursor is anchored on the endoplasmic reticulum (ER) membrane and forms a heterodimeric complex with another ER membrane-bound protein—SREBP cleavage activation protein (SCAP).[7] In response to sterol depletion, SREBP2-SCAP complex on ER membrane dissociates with ER-resident protein—insulin-induced gene (Insig), and transports from the ER membrane to Golgi where Golgi-localized Site-1 protease (S1P) and Site-2 protease (S2P) release the SREBP2 N terminus (SREBP2-N) from the membrane via proteolysis. Subsequently, SREBP2-N translocates into the nucleus to interact with the sterol regulatory element (SRE) of target genes to induce the transcription of relevant genes, leading to the increase of cholesterol synthesis.[8]

Leucine-rich repeat G-protein-coupled receptor 4 (LGR4), a member of subtype B of LGRs, is broadly expressed in cartilage, heart, hair follicle, and liver in mammals.[9,10] Its endogenous ligands have been identified to be R-spondins (Rspos), which compose of Rspo1 ~ Rspo4. Rspos-LGR4 signaling plays a pivotal role during embryogenesis as *Lgr4* null mice demonstrate severe intrauterine growth retardation and perinatal death.[11] Additionally, Rspos-LGR4 signaling is involved in multiple physiological and pathophysiological processes, such as gastrointestinal homeostasis, tumorigenesis, and food intake.[12,13] Of note, several recent studies have shed light on the probable functions of the Rspos-LGR4 axis in lipid metabolism. In skeletal muscle, *Lgr4* homozygous mutation exhibited promoted lipid oxidation under fasting condition.[14] Another study uncovers that *Lgr4* deficient mice are resistant to diet- or genetic-induced obesity due to the promotion of white-to-brown fat switch.[15] Moreover, the expression pattern of *Lgr4* in the liver exhibits a circadian rhythm. *Lgr4* homozygous mutant mice display dampened circadian rhythms of plasma triglyceride.[16] Whether Rspos-LGR4 signaling alters cholesterol metabolism remains unexplored. The present study focuses on clarifying the impact of Rspos-LGR4 signaling on hepatic cholesterol metabolism and its underlying mechanism.

2 | MATERIALS AND METHODS

2.1 | Materials

Compound C, oleic acid (OA), palmitic acid (PA), and collagenase IV were purchased from Sigma Aldrich (St. Louis, MO, USA). AICAR was purchased from MCE (NJ, USA). R-spondin 1 and R-spondin 3 were purchased from the R&D system (Minneapolis, MN). Rabbit anti-LGR4 was purchased from Santa Cruz Biotechnology (Santa Cruz, CA). Rabbit anti-AMPKα, rabbit anti-pAMPKα (Thr 172), and rabbit anti-β-catenin were purchased from Cell Signaling Technology (Beverly, MA). Rabbit anti-SREBP2, rabbit anti-AMPKα1, rabbit anti-AMPKα2 were purchased from Abcam (Cambridge, MA). Mouse anti-β-actin and mouse anti-lamin B1 were purchased from Proteintech (Chicago, USA). RNAtrip was purchased from Applygen (Beijing, China). The reverse transcription (RT) system was purchased from Invitrogen Inc (Carlsbad, CA). The nuclear protein extraction kit was purchased from BestBio (Shanghai, China). Cholesterol assay kit and triglyceride assay kit were purchased from Biosino Bio-technology & Science Inc (Beijing, China). Neofect DNA transfection reagent was purchased from Neofect Biotech (Beijing, China).

2.2 | Animals and treatments

Animals were housed in a thermostatic environment (24°C) with 12 h light and 12 h dark cycle, with access to food and water ad libitum. All experimental protocols were approved by the Animal Care and Use Committee of Peking University. *Lgr4*$^{flox/flox}$ mice were generated as described before.[16] Albumin-Cre mice (C57BL/6J background) were purchased from Jackson Laboratory (Bar Harbor, ME). Four-weeks-old *Lgr4*$^{flox/flox}$ mice were fed with normal chow diet (NCD) for 8 weeks or high-fat diet (HFD) for 12 weeks before injected with Ad-GFP or Ad-Cre (10^{10} pfu/mL) through the tail vein to knockdown hepatic *Lgr4*. After 4 d of injection, mice were sacrificed without fasting by intraperitoneal injection of pentobarbital sodium at 70 mg/kg body weight.

To generate the AL mice in which *Lgr4* is specifically deleted in hepatocytes, Albumin-Cre mice were cross-bred with *Lgr4*$^{flox/flox}$ mice. Ablation of hepatic *Lgr4* was confirmed by genotyping, quantitative RT-PCR, and Western blotting. Wild type (WT) and AL mice were fed with NCD for 8 weeks or HFD for 12 weeks before sacrifice.

2.3 | Isolation and culture of primary hepatocytes

Mice were anesthetized by intraperitoneal injection of pentobarbital sodium at 70 mg/kg body weight. 1000IU heparin was also administrated to prevent blood coagulation. After laparotomy, the portal vein was cannulated. The liver was quickly perfused with 20 mL of DHanks buffer (5 mL/min) pre-warmed in a 37°C water bath, followed by 30 mL of 0.03% pre-warmed collagenase IV (37°C) at a flow rate of 5 mL/min. Subsequently, liver was carefully removed, and hepatic tissue was dispersed into the serum-free high glucose DMEM medium. Cell suspension was then filtered through 80 μm nylon mesh, centrifuged at 50 g/min, and washed twice using the serum-free high glucose DMEM medium. Hepatocytes dispersed in high glucose DMEM medium containing 10% fetal calf serum (FBS) were counted and seeded in a 6-well plate or 12-well plate at a concentration of 0.5-1 × 10^5 cells/mL. Cells were cultured in a humid atmosphere (5% CO_2) at 37°C for 6 h to allow cell adhesion before changing to fresh high glucose DMEM medium supplemented with 10% FBS. Hepatocytes were then infected with Ad-GFP or Ad-Cre as indicated for 48 h. Where indicated, OA (125 μM) was added for 24 h, PA (300 μM) was added for 24 h, AICAR (0.5 mM) or compound C (40 μM) was supplied 1 h before harvest.

2.4 | Cell culture and shRNA transfection

AML12 cells (ATCC, Manassas, VA) were cultured in a humid atmosphere (5% CO_2) with high glucose DMEM supplemented with 10% FBS at 37°C. Cells were seeded in a 12-well plate or 6-well plate until 60%~80% confluent for transfection. The cell culture medium was replaced with 950 μL/well for the 12-well plate or 1.9 mL/well for the 6-well plate 2 h before transfection. The shRNA transfection mixture was prepared following the manufacturer's instructions. The mixture was then incubated for 18 min at 37°C and added into cells at the dose of 50 μL/well for the 12-well plate or 100 μL/well for the 6-well plate. After 36 h of incubation, the culture medium was changed into high glucose DMEM supplemented with 10% FBS. Cells were then harvested or treated with OA (125 μM, 24 h), Rspo1 (400 ng/mL, 6 h) or Rspo3 (200 ng/mL, 6 h). shRNA sequences are listed in Table S1.

2.5 | Gene expression analysis

RNA was extracted using RNAtrip and reverse-transcribed into cDNAs using the reverse transcription system. Quantitative real time-PCR based on SYBER Green was performed using the Agilent AriaMx real-time PCR system. Primer sequences used in this research are listed in Table S2.

2.6 | Western blot analysis

Cells and liver tissue were homogenized in lysis buffer. The concentration of each protein sample was determined by the BCA protein quantitative kit (Applygen, Beijing, China). Protein samples were then subjected to SDS/PAGE running gel and transferred onto nitrocellulose (NC) membrane. After incubated in 4% fat-free milk at room temperature, membranes were incubated overnight at 4°C with primary antibodies. Fluorescent secondary antibodies were used to bind with primary antibodies and visualize the expression level of specific proteins. Odyssey infrared imaging systems (LI-COR Biosciences, Lincoln, NE, USA) were used to produce the graphical view of the fluorescence signals.

2.7 | Measurement of triglyceride and cholesterol contents

About 20 mg liver tissues were homogenized in 1 mL of chloroform/methanol mix (2:1) on ice and kept at 4°C overnight to extract lipids into organic solution. Two hundred microliters of distilled water were added to the homogenates. The mixture was vortexed and centrifuged for 10 min at 3000 rpm, 4°C. The under layer was collected using injectors, followed by desiccating with nitrogen. The lyophilized powder of lipids was resolved in 5% Triton X-100 in PBS, and the supernatant was used for lipid detection. Triglyceride and cholesterol contents in liver, hepatocytes, and plasma were measured according to the manufacturer's instructions. Values were normalized to protein concentration or tissue weight.

2.8 | Oil red O staining

The oil red staining solution was prepared and filtered before using. Frozen sections of liver were prepared and rinsed in PBS for three times before fixed with 4% paraformaldehyde for 10 min. After washing in PBS, slices were incubated in the oil red staining solution for 1 h at room temperature. Subsequently, sections were counterstained with hematoxylin for 30 s and rinsed using running water for 1 h. Finally, slides were mounted using 90% glycerin for observation.

2.9 | Statistics

All data were expressed as mean ± SEM. Statistic difference was determined by two-way ANOVA and Student's *t*-test. $P < .05$ was considered significant.

3 | RESULTS

3.1 | Alteration of hepatic Rspo1/3 and LGR4 in response to energy status

To explore the functions of Rspos-LGR signaling in hepatic cholesterol metabolism, we firstly detected the expression of Rspos and LGRs subtypes in liver. As shown in Figure S1A, high levels of Rspo1 and Rspo3 were detected in liver, especially Rspo3. In contrast, levels of Rspo2 and Rspo4 were negligible. The expression of LGR4 was prominently higher than its two homologues—LGR5 and LGR6 (Figure S1A). Since liver is composed of multiple cell types, such as hepatocytes, Kupffer cells, and hepatic stellate cells, we further determined the expression of Rspos and LGR4 in different cell types. As shown in Figure S1B, both Rspo1 and Rspo3 are predominantly expressed in hepatocytes rather than Kupffer cells. Similarly, apart from hepatocytes, LGR4 was negligible in other cells such as Kupffer cells, macrophage cell line Raw264.7, and stellate cell line LX-2 (Figure S1B,C).

We next examined the alteration of hepatic Rspo1/Rspo3 and LGR4 in response to various energy statuses. Relative to the animals fed with normal chow diet (NCD), mice fed high-fat diet (HFD) showed decreased expression of *Rspo1* in liver, while the expression levels of *Rspo3* and *Lgr4* remained unaltered (Figure S1D). Consistent with the in vivo results, treating primary hepatocytes with oleic acid (OA) to mimic the in vivo positive energy balance also down-regulated *Rspo1*, while *Rspo3* and *Lgr4* were unaffected (Figure S1E). Moreover, fasting significantly up-regulated *Rspo1* in liver relative to the control fed group (Figure S1F). This change was reversed upon re-feeding (Figure S1F). *Rspo3* and *Lgr4* showed similar but less significant changes relative to *Rspo1* (Figure S1F). These results indicate that Rspos-LGR4 signaling may modulate metabolic homeostasis under different energy statuses.

3.2 | Inhibition of hepatic cholesterol synthesis by Rspo1/3

To explore the effects of Rspo1/3-LGR4 signaling on hepatic cholesterol metabolism, we treated AML12 hepatocytes with Rspo1 or Rspo3. The optimal doses of Rspo1 or Rspo3 were determined by detecting their effects on the expression of β-catenin nuclear translocation and β-catenin target genes, a well-characterized effect for Rspos-LGR4 signaling.[17] As shown in Figure S2A,B, 200 ng/mL of Rspo3, and 400 ng/mL of Rspo1 were proven to be effective. Both effective doses of Rspo1 and Rspo3 could reverse OA-induced elevation of cholesterol content (Figure 1A). However, some previous reports suggested that OA inhibits cholesterol synthesis in C6 glioma cells.[18] Therefore, we also used PA to induce the accumulation of cholesterol and found consistent results upon Rspo1 or Rspo3 stimulation (Figure S2C). Later on, we used OA to increase cholesterol content in hepatocytes. OA increased the expression of *Srebf2*—a transcription factor crucial for cholesterol synthesis, as well as its downstream target genes, that is, *Ldlr*, *Hmgcs1,* and *Hmgcr*. Importantly, Rspo1 treatment blocked the effects of OA on these genes (Figure 1B). Further, Rspo1 decreased SREBP2 nuclear translocation (Figure 1D). The effects of Rspo3 were similar to Rspo1 (Figure 1C,E). These results indicate that both Rspo1 and Rspo3 could suppress hepatic cholesterol synthesis via restraining SREBP2 transcription and nuclear translocation.

3.3 | Increment of cholesterol synthesis upon the deficiency of hepatic LGR4

To further validate the effects of Rspos-LGR4 signaling on hepatic cholesterol metabolism, we constructed $Lgr4^{flox/flox}$ mice and knocked down hepatic LGR4 through tail vein injection of Cre adenovirus (Ad-Cre). After 4 d of Ad-Cre injection, the expression of *Lgr4* in liver was significantly restrained compared with the control group injected with GFP adenovirus (Ad-GFP) (Figure S3A). We also confirmed both NCD and HFD $Lgr4^{flox/flox}$ mice displayed decreased hepatic LGR4 protein expression after Ad-Cre injection (Figure S3B). Four-weeks-old $Lgr4^{flox/flox}$ mice were fed with NCD for 8 weeks, then divided into two groups randomly and injected with Ad-GFP or Ad-Cre. Body weight and tissue weights of hepatic *Lgr4* knockdown ($Lgr4^{LKO}$) mice were unchanged relative to their littermate (Figure S3C). Histochemistry and Oil red O staining also showed no significant differences between two groups (Figure S3E,F). However, the hepatic cholesterol content of $Lgr4^{LKO}$ mice was 1.5-fold of $Lgr4^{flox/flox}$ mice (Figure 2A). No significant change in serum cholesterol, serum, and hepatic triglyceride was observed between the two groups (Figure 2A). *Srebf2* was induced in $Lgr4^{LKO}$ mice (Figure 2B). This change was associated with a significant increase of SREBP2 nuclear translocation (Figure 2E). Consistently, *Srebf2* target genes *Ldlr*, *Hmgcs1*, and *Hmgcr* were significantly up-regulated (Figure 2B).

We next examined the impacts of hepatic LGR4 deletion on cholesterol synthesis under HFD condition. Four-weeks-old $Lgr4^{flox/flox}$ mice were fed with HFD for 12 weeks, followed by Ad-Cre or Ad-GFP injection. After 4 d of injection, no significant difference was observed between $Lgr4^{flox/flox}$ and $Lgr4^{LKO}$ mice with regard to body weight and tissue weights (Figure S3D). Histochemistry and Oil red O staining showed increased lipid in the liver of $Lgr4^{LKO}$ mice compared with $Lgr4^{flox/flox}$ mice (Figure S3G,H). Consistently, hepatic cholesterol and triglyceride contents of $Lgr4^{LKO}$ mice increased by 2-folds

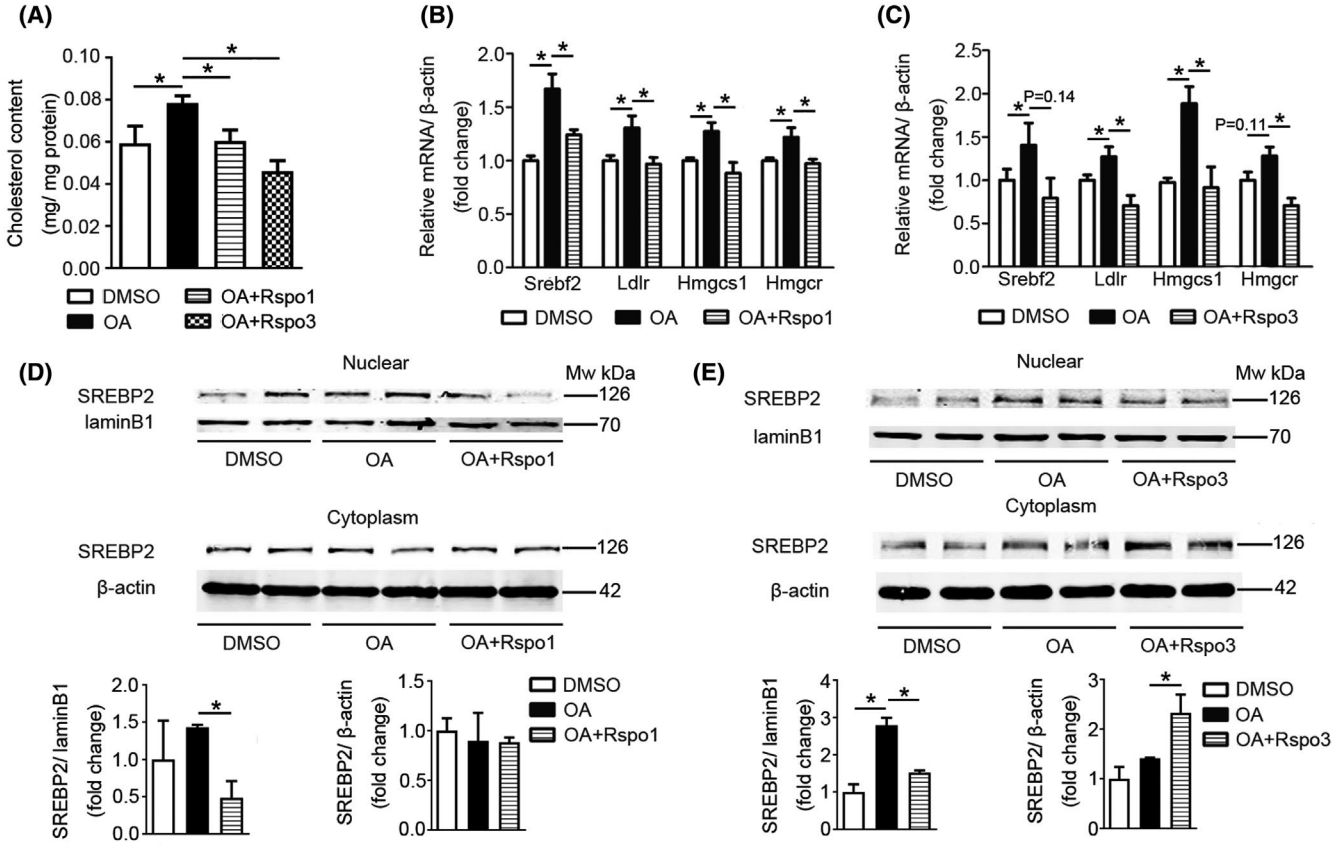

FIGURE 1 Inhibition of hepatic cholesterol synthesis by Rspo1/3. A, Cholesterol content in AML12 cells under different treatments. AML12 cells were treated with OA (125 μM) for 24 h, followed by 6 h incubation with Rspo1 or Rspo3. Cholesterol contents were determined using assay kits. n = 4. B, Rspo1 repressed expression of genes related to cholesterol uptake and synthesis upon OA treatment. Hepatic mRNAs were extracted and analyzed by quantitative RT-PCR. n = 6. C, Rspo3 repressed expression of genes related to cholesterol uptake and synthesis upon OA treatment. Hepatic mRNAs were extracted and analyzed by quantitative RT-PCR. n = 6. D, Rspo1 reversed SREBP2 nuclear translocation induced by OA. Western blotting was performed to detect the protein level of SREBP2 in the nucleus and cytoplasm. The relative expression level of SREBP2 was calculated using Image J software. Shown is the representative of at least three repeat experiments. E, Rspo3 reversed SREBP2 nuclear translocation induced by OA. Western blotting was performed to detect the protein level of SREBP2 in the nucleus and cytoplasm. The relative expression level of SREBP2 was calculated using Image J software. Shown is the representative of at least three repeat experiments. Data are represented as mean ± SEM. *$P < .05$

relative to *Lgr4*$^{flox/flox}$ mice, while serum cholesterol and triglyceride levels remained unaltered (Figure 2C). Under HFD condition, *Lgr4* deficiency resulted in an increase of *Srebf2* and its target genes, including *Ldlr*, *Hmgcs1*, and *Hmgcr* (Figure 2D). SREBP2 nuclear translocation in the liver of HFD *Lgr4*^{LKO} mice was enhanced (Figure 2F). Thus, transient ablation of hepatic *Lgr4* in mice fed either NCD or HFD enhanced the expression and nuclear translocation of *Srebf2* as well as its downstream targets, leading to a subsequent increase of cholesterol synthesis.

We next examined the effect of stable deficiency of *Lgr4* on hepatic cholesterol metabolism using the hepatic specific *Lgr4* knockout mice (AL). *Lgr4*$^{flox/flox}$ littermates (WT) were used as control. As shown in Figure S4A, body weight and most of the tissue weight were comparable between WT and AL mice fed NCD. Liver weight of AL mice slightly reduced accompanied by decreased expression of LGR4 protein in liver (Figure S4A,C). Histochemistry staining showed hepatocyte vacuolization of AL mice (Figure S4D). However, Oil red O staining was comparable between two groups (Figure S4E). Hepatic cholesterol content in AL mice elevated relative to WT mice, whereas no significant increase in hepatic triglyceride levels was observed (Figure 3A). Serum levels of cholesterol and triglyceride also increased compared with the littermates (Figure 3A). Hepatic mRNA levels of *Lgr4* decreased as expected, whereas levels of *Srebf2*, *Hmgcs1,* and *Hmgcr* significantly increased in AL mice (Figure 3B). Consistent with the change at the mRNA level, hepatic *Lgr4* ablation enhanced the translocation of SREBP2 into nuclei (Figure 3E). Similar results were observed for AL mice fed HFD. After 12 weeks of HFD, liver weight, and hepatic LGR4 expression of AL mice decreased, while body

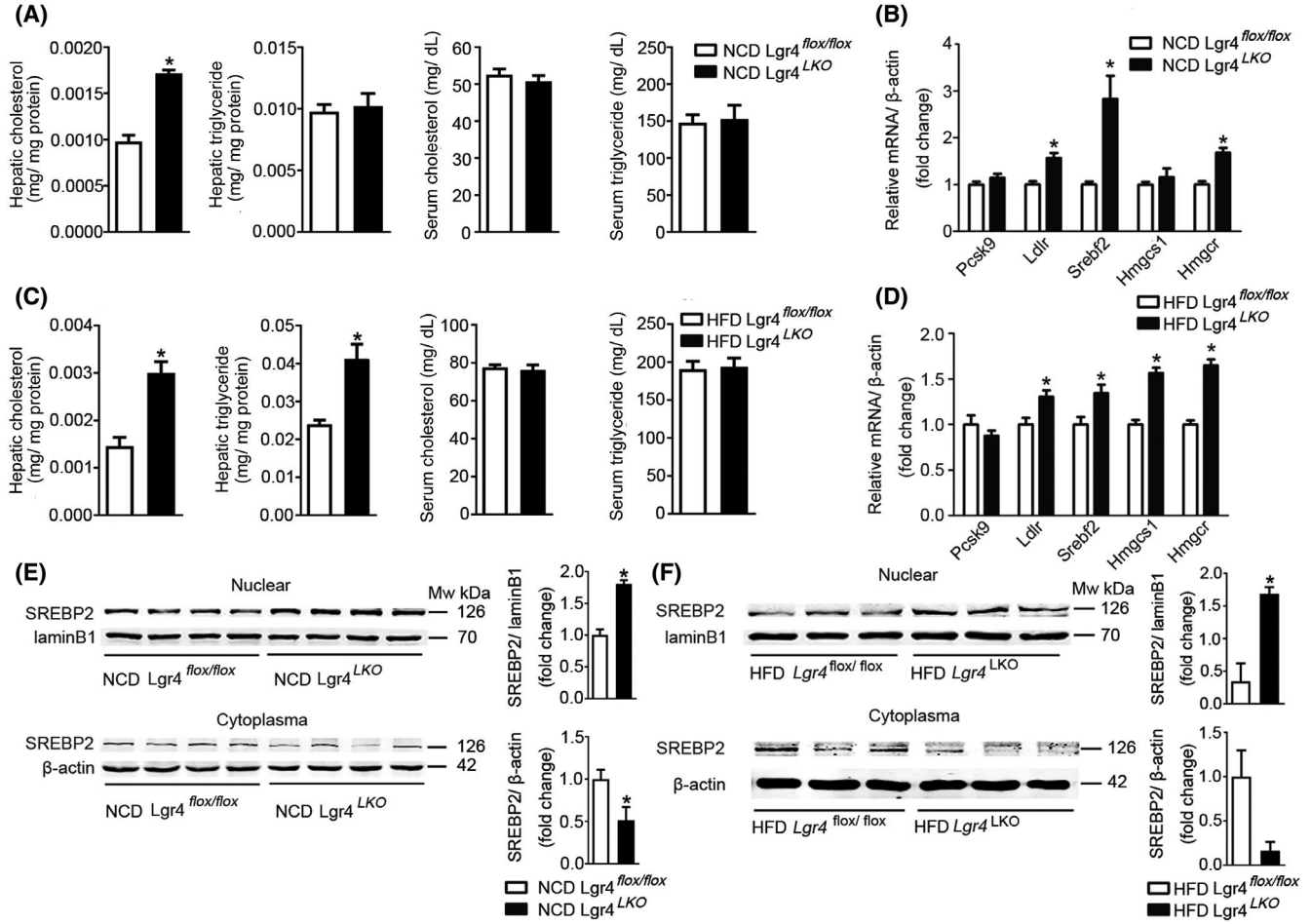

FIGURE 2 Increment of cholesterol synthesis upon hepatic LGR4 knockdown using Ad-Cre. A, NCD *Lgr4*^{LKO} mice displayed increased hepatic cholesterol content. Hepatic and serum cholesterol, triglyceride contents were measured by assay kits. n = 6. B, Upregulation of genes related to cholesterol uptake and synthesis in the liver of NCD *Lgr4*^{LKO} mice. Hepatic mRNAs were extracted and analyzed by quantitative RT-PCR. n = 6. C, Increased hepatic cholesterol and triglyceride contents in HFD *Lgr4*^{LKO} mice. Hepatic and serum triglyceride and cholesterol contents were measured by assay kits. n = 6. D, Upregulation of genes related to cholesterol uptake and synthesis in the liver of HFD *Lgr4*^{LKO} mice. Hepatic mRNAs were extracted and analyzed by quantitative RT-PCR. n = 6. E, Increased hepatic SREBP2 nuclear translocation in NCD *Lgr4*^{LKO} mice. Western blotting was performed to detect the protein level of SREBP2 in the nucleus and cytoplasm. The relative expression level of SREBP2 was calculated using Image J software. Shown is the representative of at least three repeat experiments. F, Increased hepatic SREBP2 nuclear translocation in HFD *Lgr4*^{LKO} mice. Western blotting was performed to detect the protein level of SREBP2 in the nucleus and cytoplasm. The relative expression level of SREBP2 was calculated using Image J software. Shown is the representative of at least three repeat experiments. Data are represented as mean ± SEM. *$P < .05$

weights of AL and WT mice were identical (Figure S4B,C). Although the histochemistry staining showed no significant changes, there was an increased the accumulation of perivascular lipid in the liver of AL mice (Figure S4F,G). In comparison to WT mice, AL mice demonstrated a significant increase in hepatic and serum levels of cholesterol and triglyceride (Figure 3C). Deficiency of *Lgr4* boosted the transcription of *Srebf2* (Figure 3D) and its subsequent nuclear translocation (Figure 3F) in AL mice fed HFD. Associated with the change in SREBP2, its downstream target genes significantly up-regulated, such as *Pcsk9*, *Hmgcs1,* and *Hmgcr* (Figure 3D).

In summary, either transient or stable ablation of hepatic LGR4 in mice fed NCD or HFD promotes cholesterol synthesis, SREBP2 transcription, and nuclear translocation, expression of genes relevant to cholesterol synthesis.

3.4 | Cell-autonomous effect of hepatic LGR4 deficiency

To verify that the effects of LGR4 deficiency on hepatic cholesterol synthesis are cell-autonomous, we isolated primary hepatocytes from *Lgr4*$^{flox/flox}$ mice and knocked down *Lgr4* through Ad-Cre administration. Primary hepatocytes of *Lgr4*$^{flox/flox}$ mice were treated with Ad-GFP or Ad-Cre for indicated times. After 48 h of treatment, LGR4 mRNA and protein were both effectively suppressed

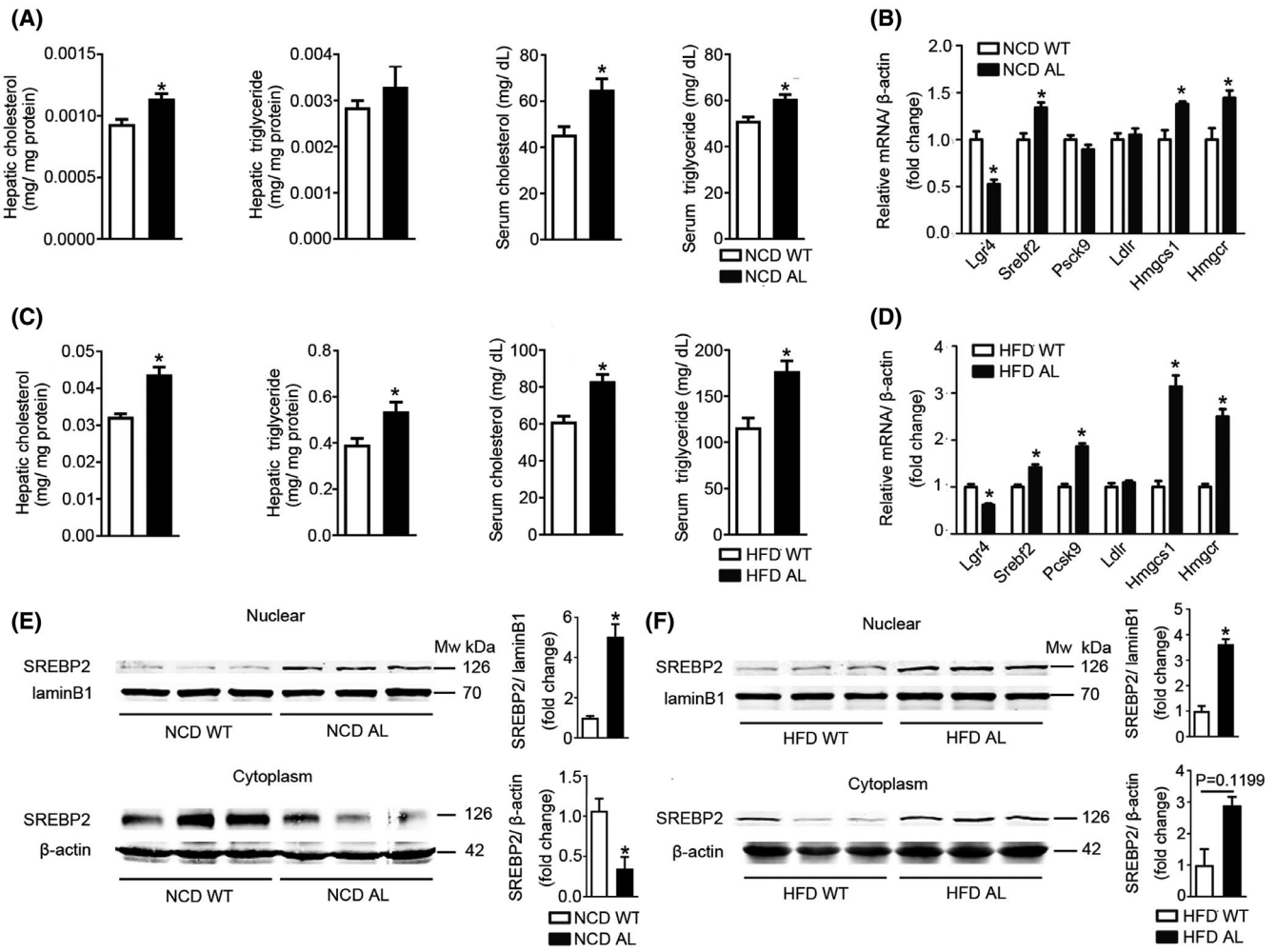

FIGURE 3 Hepatic stable deficiency of *Lgr4* promoted cholesterol synthesis. Four-weeks-old hepatic specific LGR4 deficient mice (AL mice) and their *Lgr4*$^{flox/flox}$ littermate (WT mice) were fed with normal chow diet for 8 weeks or high-fat diet for 12 weeks before sacrifice. A, Elevated hepatic cholesterol and serum cholesterol, triglyceride level of NCD AL mice compared with WT mice. Hepatic and serum cholesterol, triglyceride contents were measured by assay kits. n = 6. B, Hepatic specific *Lgr4* knockdown increased cholesterol uptake and synthesis of NCD mice. Hepatic mRNAs were extracted and analyzed by quantitative RT-PCR. n = 6. C, Elevated hepatic and serum cholesterol, triglyceride level of HFD AL mice compared with WT mice. Hepatic and serum cholesterol, triglyceride contents were measured by assay kits. n = 6. D, Hepatic specific LGR4 knockdown increased cholesterol uptake and synthesis of HFD mice. Hepatic mRNAs were extracted and analyzed by quantitative RT-PCR. n = 6. E, Hepatic specific *Lgr4* knockdown increases the nuclear translocation of SREBP2 of NCD mice. Western blotting was performed to detect the protein level of SREBP2 in the nucleus and cytoplasm. The relative expression level of SREBP2 was calculated using Image J software. Shown is the representative of at least three repeat experiments. F, Hepatic specific LGR4 knockdown increases the expression of SREBP2 of HFD mice. Western blotting was performed to detect the protein level of SREBP2 in the nucleus and cytoplasm. The relative expression level of SREBP2 was calculated using Image J software. Shown is the representative of at least three repeat experiments. Data are represented as mean ± SEM. *$P < .05$

(Figure 4A,B). LGR4 deficiency promoted cholesterol deposition in hepatocytes under conditions treated with or without OA (Figure 4C). An increase of triglyceride content in hepatocytes was only observed after OA stimulation in LGR4 deficient hepatocytes (Figure 4C). These changes were associated with an increase of genes relevant to cholesterol metabolism such as *Pcsk9*, *Ldlr*, *Srebf2*, *Hmgcs1*, and *Hmgcr* (Figure 4D). LGR4 deficient hepatocytes showed a remarkable increase of SREBP2 translocation into nuclei (Figure 4E).

3.5 | AMPKα dependent mechanism

Adenosine monophosphate (AMP)-activated protein kinase (AMPK) is one of the pivotal energy-sensing molecules expressed in almost all eukaryotic cells. Numerous studies have confirmed that AMPK is critical for cellular energy metabolism such as GLUT4 membrane translocation, fatty acid β oxidation, mitochondrial biogenesis, and autophagy.[19] Studies from ours and others have demonstrated that AMPK directly phosphorylates SREBP2 precursor, leading to the

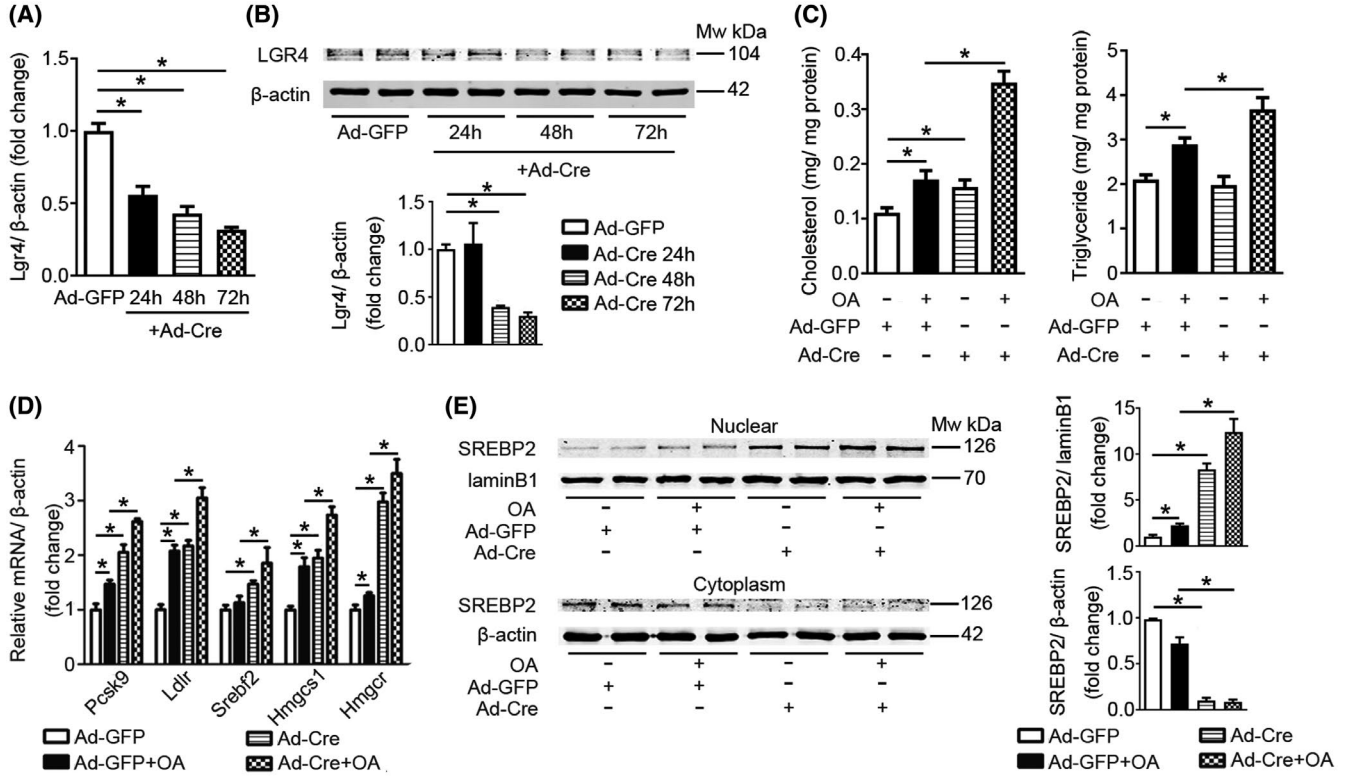

FIGURE 4 Cell-autonomous effect of hepatic LGR4 deficiency. A, Ad-Cre-induced *Lgr4* knockdown in *Lgr4*$^{flox/flox}$ primary hepatocytes. Primary hepatocytes from *Lgr4*$^{flox/flox}$ mice were isolated and infected with Ad-GFP or Ad-Cre (10^8 pfu/mL) for the indicated time. mRNAs were extracted and analyzed by quantitative RT-PCR. n = 6. B, Ad-Cre suppressed expression of LGR4 protein in *Lgr4*$^{flox/flox}$ primary hepatocytes. Western blotting was performed to detect the protein level of LGR4. The relative expression level of LGR4 was calculated using Image J software. Shown is the representative of at least three repeat experiments. C, LGR4 deficiency of hepatocytes increases cholesterol content. *Lgr4*$^{flox/flox}$ primary hepatocytes were incubated with Ad-Cre or Ad-GFP for 48 h, followed by 24 h of OA or DMSO treatment. Cholesterol and triglyceride content in hepatocytes were then determined after different treatments by assay kits. n = 6. D, LGR4 deficiency of hepatocytes increases cholesterol uptake and synthesis. After indicated treatments, mRNA was extracted from primary hepatocytes and analyzed by quantitative RT-PCR. n = 6. E, LGR4 deficiency of hepatocytes increases the nuclear translocation of SREBP2. After indicated treatments, western blotting was performed to detect the protein level of SREBP2 in the nucleus and cytoplasm. The relative expression level of SREBP2 was calculated using Image J software. Shown is the representative of at least three repeat experiments. Data are represented as mean ± SEM. *$P < .05$

reduction of SREBP2 nuclear translocation.[6,20,21] We thus examined the effects of Rspo1/3-LGR4 signaling on AMPK. As shown in Figure 5A, both Rspo1 and Rspo3 stimulation potentiated the phosphorylation of Thr172 site of AMPKα in AML12 cells, indicating AMPK activation. Compound C is commonly used as an AMPK antagonist. As presented in Figure S5A, incubation of AML12 cells with compound C for 1 h dose-dependently reduced the phosphorylation of AMPKα Thr172. Rspo1 and Rspo3 significantly attenuated OA-induced elevation of the cholesterol content in AML12 cells (Figure 5B). This effect was blunted by compound C (Figure 5B). Compound C significantly attenuated the Rspo1-induced activation of AMPKα and subsequent suppression of cholesterol metabolism relevant genes including *Srebf2*, *Ldlr*, *Hmgcs1*, and *Hmgcr*, as well as the nuclear translocation of SREBP2 in hepatocytes treated with OA (Figure 5C,D). Similarly, compound C abolished the effects of Rspo3 on AMPKα, cholesterol metabolism relevant genes, and the SREBP2 nuclear translocation (Figure 5E,F).

In *Lgr4*$^{flox/flox}$ mice fed NCD and HFD, transient knockdown of hepatic LGR4 using Ad-Cre resulted in reduced activation of AMPKα (Figure 6A). Similarly, the phosphorylation of AMPKα in liver with stable deletion of LGR4 (AL mice) significantly declined compared with WT mice (Figure 6A). In vitro, knockdown LGR4 in *Lgr4*$^{flox/flox}$ hepatocytes using Ad-Cre suppressed activation of AMPKα as well (Figure 6B). We then tested if AMPKα agonist AICAR could reverse the changes driven by LGR4 depletion. In AML12 cells, AICAR dose-dependently potentiated AMPKα phosphorylation at the Thr172 site (Figure S5B). Activation of AMPKα by AICAR significantly attenuated the increase of hepatic cholesterol content in LGR4 deficient hepatocytes treated with or without OA (Figure 6C). Consistently, AICAR abolished the up-regulation of *Srebf2* and its target genes including *Ldlr*, *Hmgcs1*, and *Hmgcr* induced by LGR4 deletion (Figure 6D). Additionally, AICAR treatment was sufficient to block the SREBP2 nuclear translocation induced by LGR4 ablation (Figure 6E).

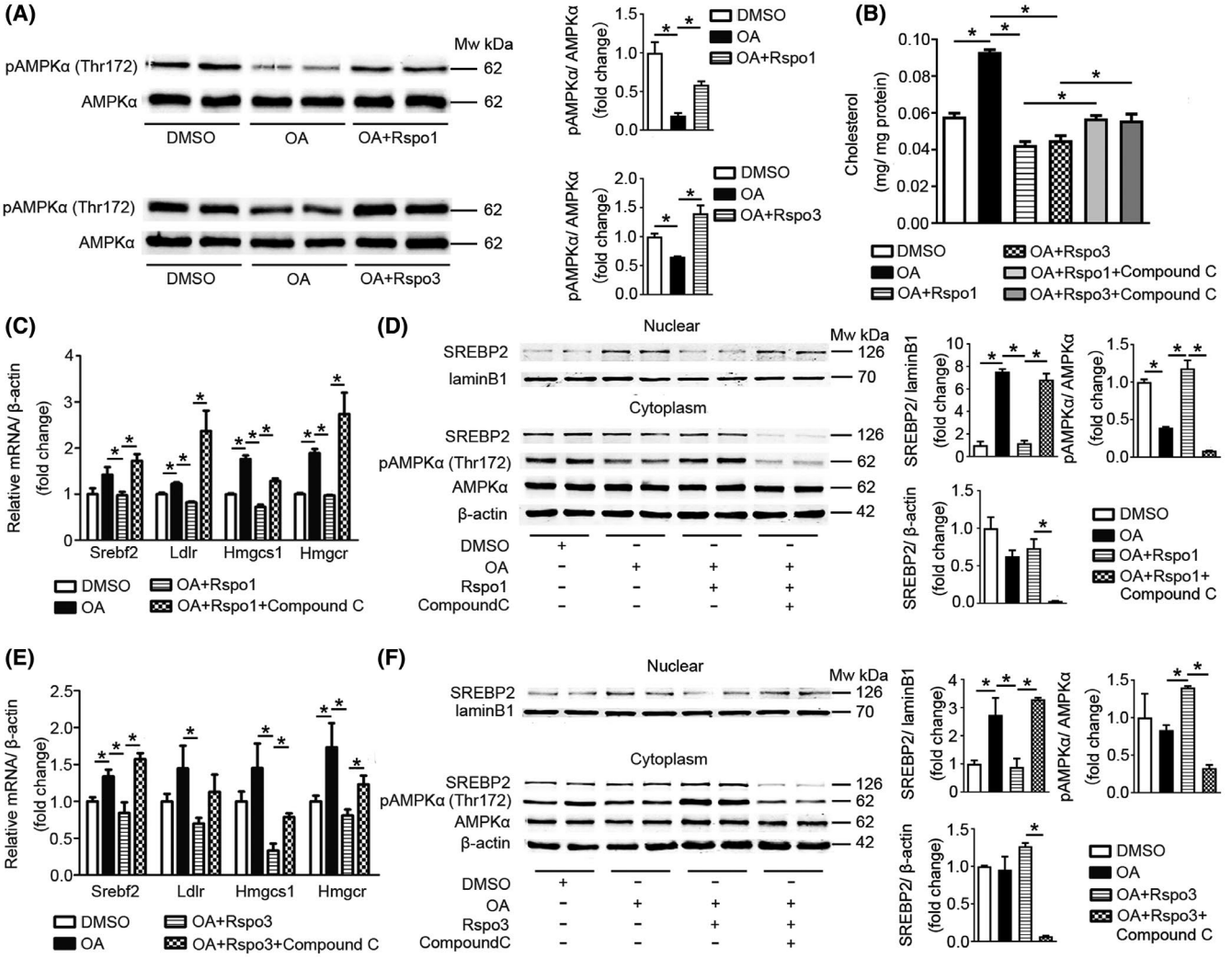

FIGURE 5 Rspo1/3 inhibits cholesterol synthesis through activating AMPKα. A, Rspo1/3 promoted activation of AMPKα. AML12 cells were treated with OA for 24 h and then incubated with Rspo1/Rspo3 for 6 h. Western blotting was performed to detect protein levels. The relative expression levels of proteins were calculated using Image J software. Shown is the representative of at least three repeat experiments. B, Compound C diminished the inhibitory effects of Rspo1/3 on cholesterol accumulation. AML12 cells were treated with OA for 24 h, followed by Rspo1/Rspo3 for 6 h. Afterward, AML12 cells were incubated with compound C (40 μM) for 1 h. Cholesterol contents in hepatocytes were then determined by assay kits. n = 4. C, Compound C diminishes the inhibitory effects of Rspo1 on cholesterol uptake and synthesis. After indicated treatments, mRNA was extracted from hepatocytes and analyzed by quantitative RT-PCR. n = 6. D, Compound C diminishes the inhibitory effects of Rspo1 on the nuclear translocation of SREBP2. Western blotting was performed to detect protein levels. The relative expression levels of proteins were calculated using Image J software. Shown is the representative of at least three repeat experiments. E, Compound C diminishes the inhibitory effects of Rspo3 on cholesterol uptake and synthesis. After indicated treatments, mRNA was extracted from hepatocytes and analyzed by quantitative RT-PCR. n = 6. F, Compound C diminishes the inhibitory effects of Rspo3 on the nuclear translocation of SREBP2. Western blotting was performed to detect protein levels. The relative expression levels of proteins were calculated using Image J software. Shown is the representative of at least three repeat experiments. Data are represented as mean ± SEM. *$P < .05$

Two isoforms of AMPKα have been identified to date, namely, AMPKα1 and AMPKα2.[22] To explore the isoform mediating the downstream effects of Rspo1/3-LGR4 signaling, we constructed shRNA specifically interfering AMPKα1 or AMPKα2. AML12 cells transfected with AMPKα1 shRNA for 36 h demonstrated a significant reduction in the levels of AMPKα1, while AMPKα2 levels were unaffected (Figure 7A). Remarkably, AMPKα1 deficiency abrogated the inhibitory effects of Rspo1 on cholesterol synthesis (Figure 7A), mRNA levels of *Srebf2*, *Ldlr*, *Hmgcs1*, and *Hmgcr* (Figure 7B), as well as the nuclear translocation of SREBP2 (Figure 7C). AMPKα1 deficiency reduced the Rspo1-induced upregulation of AMPKα phosphorylation (Figure 7C). Similar results were also found upon Rspo3 stimulation (Figure S6A-C).

As shown in Figure 7D, AML12 cells transfected with AMPKα2 shRNA for 36 h significantly reduced the expression level of AMPKα2 without affecting AMPKα1. Much

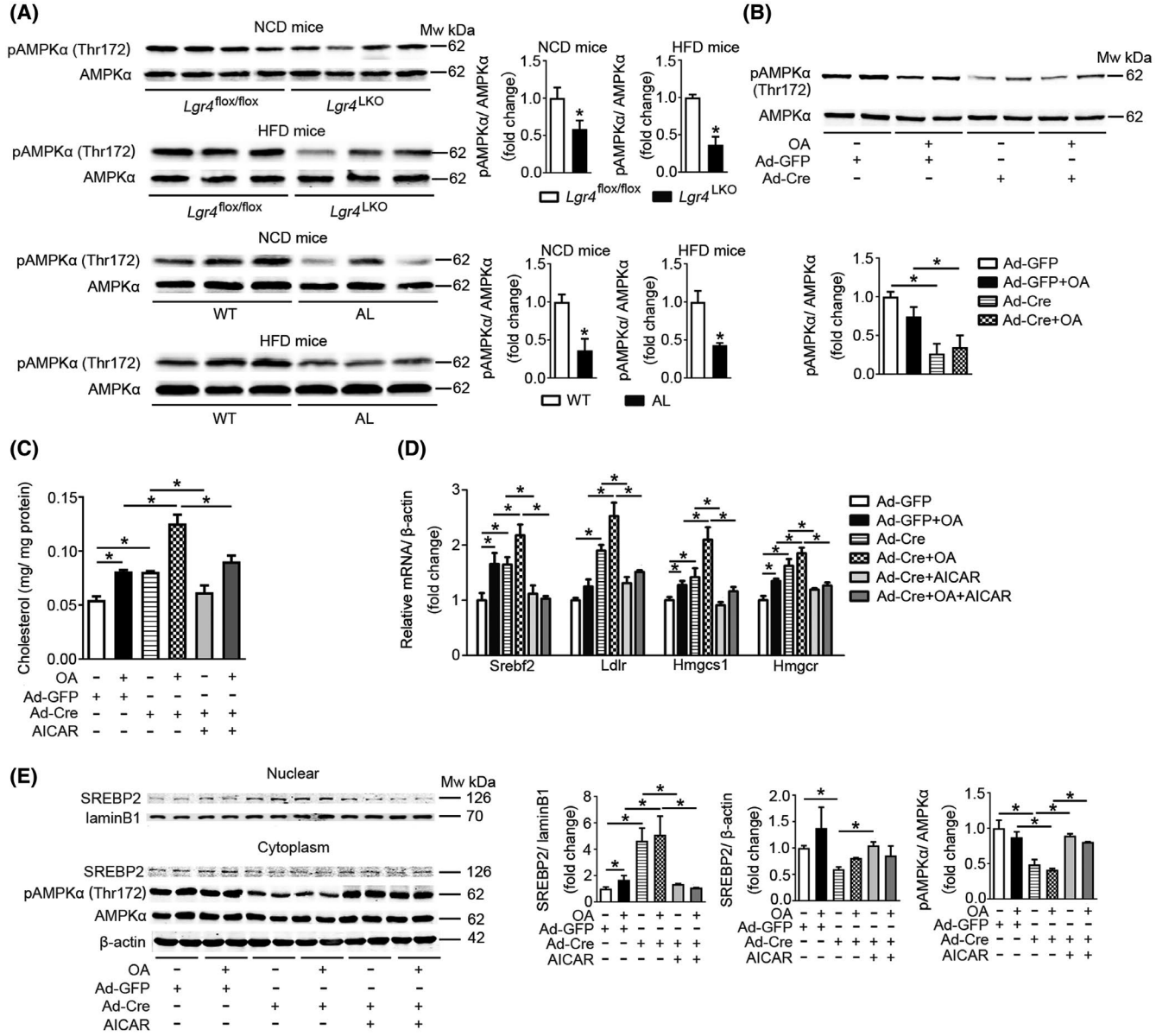

FIGURE 6 LGR4 ablation promotes cholesterol synthesis through inhibiting AMPKα. A, Transient and stable hepatic LGR4 knockdown repressed AMPKα activation. Western blotting was performed to detect the level of AMPKα phosphorylation in liver. The relative expression levels of proteins were calculated using Image J software. Shown is the representative of at least three repeat experiments. B, LGR4 depletion suppressed AMPKα activation in hepatocytes. Western blotting was performed to detect the level of AMPKα phosphorylation in *Lgr4*$^{flox/flox}$ primary hepatocytes after indicated treatment. The relative expression levels of proteins were calculated using Image J software. Shown is the representative of at least three repeat experiments. C, AICAR reversed LGR4 knockdown-induced cholesterol accumulation. *Lgr4*$^{flox/flox}$ primary hepatocytes were incubated with Ad-Cre or Ad-GFP for 48 h, followed by AICAR (0.5 mM) treatment for 1 h. Cholesterol contents in hepatocytes of different treatments were then determined by assay kits. n = 4. D, AICAR reversed LGR4 knockdown-induced cholesterol uptake and synthesis. After indicated treatments, mRNA was extracted from hepatocytes and analyzed by quantitative RT-PCR. E, AICAR reversed LGR4 knockdown-induced nuclear translocation of SREBP2. Western blotting was performed to detect protein levels. The relative expression levels of proteins were calculated using Image J software. Shown is the representative of at least three repeat experiments. Data are represented as mean ± SEM. *$P < .05$

alike AMPKα1 knockdown, AMPKα2 deletion also reversed the decrease of cholesterol level (Figure 7D), mRNA levels of cholesterol metabolism relevant genes such as *Srebf2*, *Ldlr*, *Hmgcs1*, and *Hmgcr* (Figure 7E), and nuclear translocation of SREBP2 (Figure 7F) in hepatocytes treated with Rspo1. The silence of the AMPKα2 gene significantly attenuated the increase of AMPKα phosphorylation induced by Rspo1 (Figure 7F). Much like Rspo1, AMPKα2 knockdown hepatocytes displayed similar results under Rspo3 treatment (Figure S6D-F).

Hepatocytes with double-knockdown of AMPKα1 and AMPKα2 were resistant to Rspo1 or Rspo3 induced the

decline of cholesterol level (Figure S7A,B). The effects of Rspo1 and Rspo3 on cholesterol metabolism relevant genes such as *Srebf2*, *Ldlr*, *Hmgcs1*, *Hmgcr* were significantly blunted in hepatocytes with ablation of both AMPKα1 and AMPKα2 (Figure S7C,D). Likewise, the inhibitory effects of Rspo1 and Rspo3 on SREBP2 nuclear translocation were

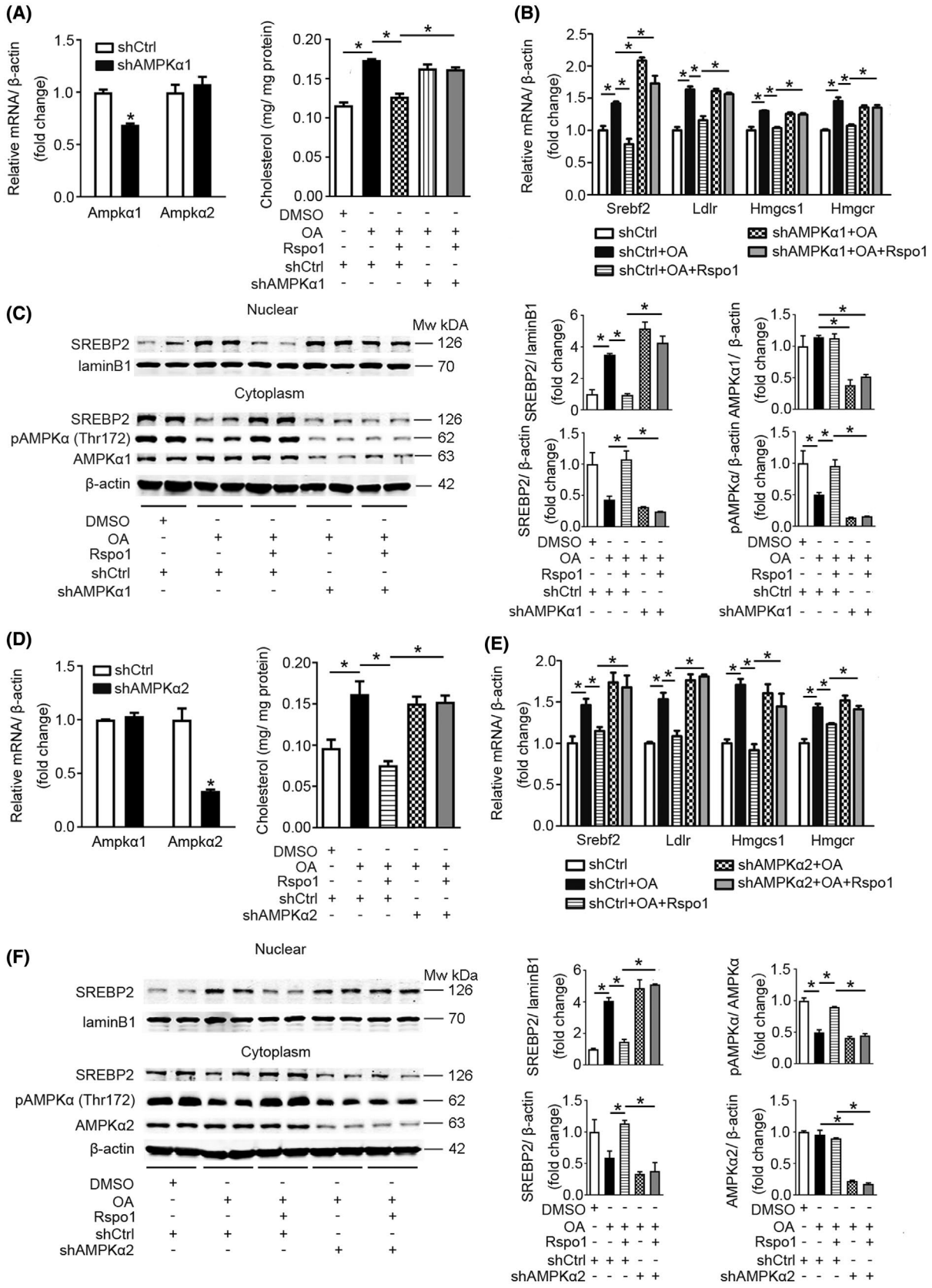

FIGURE 7 AMPKα1/2 knockdown abolished the inhibitory effects of Rspo1-LGR4 signaling on hepatic cholesterol synthesis. A, AMPKα1 knockdown diminishes the inhibitory effects of Rspo1 on cholesterol accumulation. AML12 cells were transfected with AMPKα1 shRNA for 36 h. mRNA was extracted from hepatocytes and analyzed by quantitative RT-PCR. n = 6. *$P < .05$ vs shCtrl. After the transfection, cells were treated by OA for 24 h and stimulated by Rspo1 for 6 h. Cholesterol contents in hepatocytes after different treatments were determined by assay kits. n = 4. B, AMPKα1 knockdown reversed Rspo1-induced downregulation of genes related to cholesterol uptake and synthesis. After indicated treatments, mRNA was extracted from hepatocytes and analyzed by quantitative RT-PCR. C, AMPKα1 knockdown diminishes the inhibitory effects of Rspo1 on the nuclear translocation of SREBP2. Western blotting was performed to detect protein levels. The relative expression levels of proteins were calculated using Image J software. Shown is the representative of at least three repeat experiments. D, AMPKα2 knockdown diminishes the inhibitory effects of Rspo1 on cholesterol accumulation. AML12 cells were transfected with AMPKα2 shRNA for 36 h, mRNA was extracted from hepatocytes and analyzed by quantitative RT-PCR. n = 6. *$P < .05$ vs shCtrl. After the transfection, cells were treated by OA for 24 h and stimulated by Rspo1 for 6 h. Cholesterol contents in hepatocytes after different treatments were determined by assay kits. n = 4. E, AMPKα2 knockdown reversed Rspo1-induced downregulation of genes related to cholesterol uptake and synthesis. After indicated treatments, mRNA was extracted from hepatocytes and analyzed by quantitative RT-PCR. n = 6. F, AMPKα2 knockdown diminishes the inhibitory effects of Rspo1 on the nuclear translocation of SREBP2. Western blotting was performed to detect protein levels. The relative expression levels of proteins were calculated using Image J software. Shown is the representative of at least three repeat experiments. Data are represented as mean ± SEM. *$P < .05$

apparently abolished in hepatocytes with deficiency of both AMPKα1 and AMPKα2 (Figure S7E,F).

4 | DISCUSSION

Rspos-LGR4 signaling has been demonstrated to be critical for embryogenesis and maintenance of stem cell functions. The present study reveals a pivotal role for this signaling pathway in the cholesterol homeostasis. The highlights of our study are as follows: (a) Rspo1/3 inhibits hepatic cholesterol synthesis, while LGR4 deficiency increases cholesterol contents in hepatocytes; (b) Rspo1/3 activates AMPKα, and subsequently blocks the transcriptional activation of *Srebf2* and the SREBP2 nuclear translocation, leading to the suppression of its target genes involved in cholesterol synthesis, while the deletion of hepatic LGR4 induced opposite effects; (c) Both pharmacological or genetic intervention of AMPKα reverse the inhibitory effects of Rspo1 and Rspo3 on hepatic cholesterol synthesis. Our study thus demonstrates that Rspo1/3-LGR4 signaling inhibits hepatic cholesterol synthesis through a mechanism dependent on the AMPK-SREBP2 pathway (Figure 8).

Being mainly expressed in the stem cells, LGR4 is critical for the maintenance of stem cells and thus for the embryonic development.[11] Our finding extends the physiological function of LGR4 to the cholesterol homeostasis. Conflicting results have been reported on the metabolic

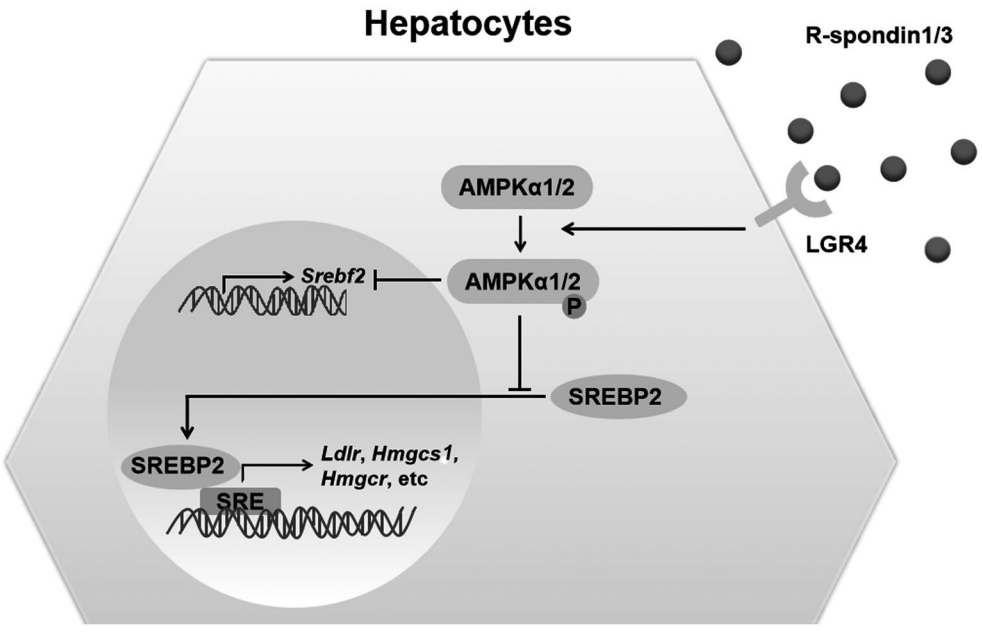

FIGURE 8 Schematic diagram showing the mechanism by which Rspo1/Rspo3- LGR4 signaling inhibits hepatic cholesterol synthesis. In hepatocytes, Rspo1/3 bind to their receptor LGR4 to promote phosphorylate of AMPKα. The activated AMPKα will further restrain the expression and nuclear translocation of SREBP2; therefore, downregulate transcription of genes related to cholesterol uptake and synthesis, including *Ldlr*, *Hmgcs1*, and *Hmgcr*

function of LGR4. In the hypothalamus, activation of LGR4 by R-spondin 1 or 3 inhibits food intake.[23] In contrast, mice with global ablation of LGR4 show decrement in adiposity and resistance to dietary and leptin mutant-induced obesity, due to enhanced browning of white adipose tissues.[14] Consistently, human genetic analysis has identified the gain-of-function variant of LGR4, LGR4 A750T variant, as a genetic determinant of central obesity.[24] All these studies suggest that LGR4 may either function as an anorexic signal through the central hypothalamus or as a stimulator for energy expenditure through peripheral adipose tissues to promote negative or positive energy balance, respectively. Thus, conditional manipulation of LGR4 in distinct cells such as hypothalamic neurons, adipocytes, hepatocytes, and islet cells is a critical precondition to dissect the differential action of this molecule on energy homeostasis. Using the in vivo and in vitro approach to specifically manipulate the expression of the LGR4 gene in hepatocytes, we reveal an additional physiological function for LGR4 in cholesterol metabolism. Activation of LGR4 in hepatocytes by R-spondin 1 or 3 attenuated cholesterol synthesis, whereas deficiency of LGR4 in hepatocytes significantly increased the synthesis of cholesterol both in mice and in cultured hepatocytes. The reduction of hepatic cholesterol upon the activation of LGR4 may occur through the attenuation of cholesterol synthesis. Our study thus establishes Rspo1/3-LGR4 signaling as a novel endogenous system contributing to the cholesterol homeostasis. Targeting the Rspos-LGR4 signaling in hepatocytes may provide an alternative strategy for the intervention of cholesterol dysfunction including hypercholesterolemia.

The intracellular signaling pathway mediating the physiological function of Rspos-LGR4 remains largely unknown. Previous study has suggested that Rspos-LGR4 functions to potentiate Wnt/β-catenin signaling.[17] We have identified AMPKα-SREBP2 as the downstream mediators of Rspo1/3-LGR4 signaling in the control of hepatic cholesterol synthesis. Both pharmacological and genetic intervention of AMPKα reversed the decrement of SREBP2 nuclear translocation induced by Rspo1/3 and suppressed cholesterol synthesis. Conversely, AMPKα agonist abolished the enhancement of cholesterol synthesis in the context of LGR4 ablation. Furthermore, both isoforms of AMPKα are required for the suppression of hepatic cholesterol synthesis induced by Rspo1/3-LGR4 signaling.

How Rspo1/3-LGR4 signaling activates AMPKα remains unclear. Having been extensively verified, the major function of the Rspos-LGR4 pathway is to potentiate Wnt/β-catenin signaling. Accordingly, we assume that the Wnt/β-catenin axis may be responsible for the ectopic activation of AMPKα. Glycogen synthase kinase 3β (GSK3β) negatively regulates Wnt/β-catenin signaling through accelerating the degradation of β-catenin. Previous studies have demonstrated that GSK3β acts as a potent inhibitor of AMPK activation.[25,26] Further study is required to determine whether GSK3β is involved in Rspos-LGR4 stimulated AMPK phosphorylation in hepatocytes.

In summary, our study demonstrates that in liver, Rspos-LGR4 signaling functions as a crucial endogenous pathway to inhibit cholesterol synthesis through suppressing SREBP2 as well as its downstream targets. This function of the Rspos-LGR4 axis is mediated by AMPKα. Considering that the elevation of cholesterol in liver is critical for the progression from NAFL to NASH, our finding suggests that the Rspos-LGR4 axis may provide novel therapeutic targets for NAFLD.

ACKNOWLEDGMENTS

This research was supported by grants from the National Key R&D Program of China (2017YFC0908900), the National Natural Science Foundation of China (81730020, 81930015), and National Institutes of Health Grant 1R01DK110273 and R01DK112755.

CONFLICT OF INTEREST

Authors declare no conflicts of interest.

AUTHOR CONTRIBUTIONS

S. Liu, Y. Yin, and W. Zhang designed the research; S. Liu, Y. Gao, and L. Zhang performed the research; S. Liu and Y. Gao analyzed the data; S. Liu drafted the paper; S. Liu, Y. Yin, and W. Zhang revised the paper.

REFERENCES

1. Masuoka HC, Chalasani N. Nonalcoholic fatty liver disease: an emerging threat to obese and diabetic individuals. *Ann N Y Acad Sci*. 2013;1281:106-122.
2. Min HK, Kapoor A, Fuchs M, et al. Increased hepatic synthesis and dysregulation of cholesterol metabolism is associated with the severity of nonalcoholic fatty liver disease. *Cell Metab*. 2012;15:665-674.
3. Puri P, Baillie RA, Wiest MM, et al. A lipidomic analysis of nonalcoholic fatty liver disease. *Hepatology*. 2007;46:1081-1090.
4. Dongiovanni P, Petta S, Mannisto V, et al. Statin use and non-alcoholic steatohepatitis in at risk individuals. *J Hepatol*. 2015;63:705-712.
5. Yoneda M, Fujita K, Nozaki Y, et al. Efficacy of ezetimibe for the treatment of non-alcoholic steatohepatitis: an open-label, pilot study. *Hepatol Res*. 2010;40:566-573.
6. Tang H, Yu R, Liu S, Huwatibieke B, Li Z, Zhang W. Irisin inhibits hepatic cholesterol synthesis via AMPK-SREBP2 signaling. *EBioMedicine*. 2016;6:139-148.
7. Goldstein JL, DeBose-Boyd RA, Brown MS. Protein sensors for membrane sterols. *Cell*. 2006;124:35-46.
8. Nagoshi E, Imamoto N, Sato R, Yoneda Y. Nuclear import of sterol regulatory element-binding protein-2, a basic helix-loop-helix-leucine zipper (bHLH-Zip)-containing transcription factor, occurs through the direct interaction of importinβ with HLHZip. *Mol Biol Cell*. 1999;10:2221-2233.

9. Yi J, Xiong W, Gong X, Bellister S, Ellis LM, Liu Q. Analysis of LGR4 receptor distribution in human and mouse tissues. *PLoS One*. 2013;8:e78144.
10. Mazerbourg S, Bouley DM, Sudo S, et al. Leucine-rich repeat-containing, G protein-coupled receptor 4 null mice exhibit intrauterine growth retardation associated with embryonic and perinatal lethality. *Mol Endocrinol*. 2004;18:2241-2254.
11. Li Z, Zhang W, Mulholland MW. LGR4 and its role in intestinal protection and energy metabolism. *Front Endocrinol*. 2015;6:131.
12. Gao Y, Kitagawa K, Hiramatsu Y, et al. Up-regulation of GPR48 induced by down-regulation of p27Kip1 enhances carcinoma cell invasiveness and metastasis. *Cancer Res*. 2006;66:11623-11631.
13. Sun Y, Hong J, Chen M, et al. Ablation of Lgr4 enhances energy adaptation in skeletal muscle via activation of Ampk/Sirt1/Pgc1α pathway. *Biochem Biophys Res Commun*. 2015;464:396-400.
14. Wang J, Liu R, Wang F, et al. Ablation of LGR4 promotes energy expenditure by driving white-to-brown fat switch. *Nat Cell Biol*. 2013;15:1455-1463.
15. Wang F, Zhang X, Wang J, et al. LGR4 acts as a link between the peripheral circadian clock and lipid metabolism in liver. *J Mol Endocrinol*. 2014;52:133-143.
16. Li Z, Liu S, Lou J, Mulholland M, Zhang W. LGR4 protects hepatocytes from injury in mouse. *Am J Physiol Gastrointest Liver Physiol*. 2019;316:G123-G131.
17. de Lau W, Peng WC, Gros P, Clevers H. The R-spondin/Lgr5/Rnf43 module: regulator of Wnt signal strength. *Genes Dev*. 2014;28:305-316.
18. Natali F, Siculella L, Salvati S, Gnoni GV. Oleic acid is a potent inhibitor of fatty acid and cholesterol synthesis in C6 glioma cells. *J Lipid Res*. 2007;48:1966-1975.
19. Hardie DG, Ross FA, Hawley SA. AMPK: a nutrient and energy sensor that maintains energy homeostasis. *Nat Rev Mol Cell Biol*. 2012;13:251-262.
20. Li Y, Xu S, Mihaylova MM, et al. AMPK phosphorylates and inhibits SREBP activity to attenuate hepatic steatosis and atherosclerosis in diet-induced insulin-resistant mice. *Cell Metab*. 2011;13:376-388.
21. Liu S, Jing F, Yu C, Gao L, Qin Y, Zhao J. AICAR-induced activation of AMPK inhibits TSH/SREBP-2/HMGCR pathway in liver. *PLoS One*. 2015;10:e0124951.
22. Hardie DG. AMP-activated/SNF1 protein kinases: conserved guardians of cellular energy. *Nat Rev Mol Cell Biol*. 2007;8:774-785.
23. Li JY, Chai B, Zhang W, Fritze DM, Zhang C, Mulholland MW. LGR4 and its ligands, R-spondin 1 and R-spondin 3, regulate food intake in the hypothalamus of male rats. *Endocrinology*. 2014;155:429-440.
24. Zou Y, Ning T, Shi J, et al. Association of a gain-of-function variant in LGR4 with central obesity. *Obesity*. 2017;25:252-260.
25. Zhou H, Wang H, Ni M, et al. Glycogen synthase kinase 3β promotes liver innate immune activation by restraining AMP-activated protein kinase activation. *J Hepatol*. 2018;69:99-109.
26. Suzuki T, Bridges D, Nakada D, et al. Inhibition of AMPK catabolic action by GSK3. *Mol Cell*. 2013;50:407-419.

SUPPORTING INFORMATION

Additional supporting information may be found online in the Supporting Information section.

How to cite this article: Liu S, Gao Y, Zhang L, Yin Y, Zhang W. Rspo1/Rspo3-LGR4 signaling inhibits hepatic cholesterol synthesis through the AMPKα-SREBP2 pathway. *The FASEB Journal*. 2020;34:14946–14959. https://doi.org/10.1096/fj.202001234R